Multiphoton Tomography and Cross-Polarization Optical Coherence Tomography for Diagnosing Brain Gliomas: Pilot Study

DOI: 10.17691/stm2016.8.4.09
Received May 30, 2016

© **V.V. Dudenkova,** Junior Researcher, Laboratory of Studying Optical Structure of Biotissues, Institute of Biomedical Technologies[1]; PhD Student, Faculty of Radiophysics[2];
K.S. Yashin, PhD Student, Department of Neurosurgery[3]; Junior Researcher, Laboratory of High-Resolution Microscopy and Gene Technology, Institute of Biomedical Technologies[1];
E.B. Kiseleva, PhD, Researcher, Laboratory of Studying Optical Structure of Biotissues, Institute of Biomedical Technologies[1];
S.S. Kuznetsov, MD, DSc, Professor, Department of Pathological Anatomy[1];
L.B. Timofeeva, PhD, Assistant, Department of Histology with Cytology and Embryology[1];
A.S. Khalansky, MD, PhD, Head of the Laboratory of Experimental Histopathology of Central Nervous System[4];
V.V. Elagin, Researcher, Laboratory of Studying Optical Structure of Biotissues, Institute of Biomedical Technologies[1];
E.V. Gubarkova, PhD, Junior Researcher, Laboratory of Studying Optical Structure of Biotissues, Institute of Biomedical Technologies[1];
M.M. Karabut, Junior Researcher, Laboratory of Studying Optical Structure of Biotissue, Institute of Biomedical Technologies[1];
N.P. Pavlova, Laboratory Technician, Laboratory of Studying Optical Structure of Biotissue, Institute of Biomedical Technologies[1],
I.A. Medyanik, MD, PhD, Senior Researcher, Group Microneurosurgery[3];
L.Ya. Kravets, MD, DSc, Professor, Chief Researcher, Group Microneurosurgery[3];
N.D. Gladkova, MD, DSc, Professor, Vice Director for Science, Institute of Biomedical Technologies[1]

[1]Nizhny Novgorod State Medical Academy, 10/1 Minin and Pozharsky Square, Nizhny Novgorod, 603005, Russian Federation;
[2]Nizhny Novgorod Regional Oncologic Hospital, 190 Rodionova St., Nizhny Novgorod, 603126, Russian Federation;
[3]Privolzhsky Federal Research Medical Centre, Ministry of Health of the Russian Federation, 18 Verkhne-Volzhskaya naberezhnaya St., Nizhny Novgorod, 603155, Russian Federation;
[4]Research Institute of Human Morphology, 3 Zurupy St., Moscow, 117418, Russian Federation

Progress in the surgery of infiltratively growing gliomas is closely related to intraoperative diagnostics. Currently the most promising methods of optical imaging in the field of intraoperative identification of glioma boundaries and of grade of tumor are those providing high spatial resolution, such as optical coherence tomography (OCT) and multiphoton tomography (MPT). Nevertheless, for routine clinical use, evidence-based criteria are required. In this work the results of parallel *ex vivo* analysis of specimens of different grades of gliomas and of peritumoral areas obtained through the use of MPT and cross-polarization OCT (CP OCT) are compared with simultaneous histological descriptions and are presented in order to reveal the usefulness of each method in neurooncology.

Key words: multiphoton tomography (MPT); cross-polarization optical coherence tomography (CP OCT); brain tumor rat model; glioma; glioblastoma; intraoperative diagnostics.

Gliomas constitute a considerable part (34%) of all intracranial tumors in people aged over 18 [1, 2]. Their distinctive feature is infiltrative growth into the surrounding white matter of the brain making it difficult to differentiate the boundary between the tumor and the brain tissue. According to the growth rate and the degree of invasion, astrocytic tumors are conditionally divided into slow-growing and fast-growing ones. The first group consists of pilocytic astrocytomas (Grade I) and diffuse astrocytomas (Grade II), while the latter types are anaplastic astrocytomas (Grade III) and glioblastomas (Grade IV) [3]. The higher the degree of malignancy, the more aggressive are both the tumor growth and the nature of invasion.

For contacts: Konstantin S. Yashin, e-mail: jashinmed@gmail.com

The main paradigm of glial tumor surgery today is maximum resection while minimizing the risk of damaging eloquent areas of the brain [4]. The size of the tumor resection is a key predictor that directly and reliably correlates with the patients' life expectancy [4–12]. However, total resection of a tumor is almost impossible in practice because there is no distinct boundary between the normal brain tissue and the tumor. Thus, traditional excision of a tumor under a white light microscope enables maximum resection in only 25–30% of cases due to the low resolution [8, 9, 13]. Currently used technologies such as intraoperative MPT (resolution is about 1 mm) and fluorescence diagnostics significantly enhance opportunities for the neurosurgeon [14]. However, these methods are limited in their determination of the boundaries of tumor invasion because they also lack sufficient resolution.

Today the most promising methods are optical bioimaging, with spatial resolutions of about 1 μm. Confocal microscopy [15], multiphoton tomography (MPT) [16] and optical coherence tomography (OCT) [17, 18] are of interest not only in respect of intraoperative identification of neoplasm boundaries, but also as methods for optical cytobiopsy.

Multiphoton microscopy (or multiphoton laser-scanning microscopy, MPM) is a modern method of fluorescence imaging applied for *in vivo* studies. As an excitation source, a femtosecond pulsed infrared laser is used, allowing simultaneous visualization of the tissues using several modes i.e. the second harmonic generation (SHG) from anisotropic structures, and in two-photon-excited autofluorescence (TPEF or 2PEF) mode with spectral detection of the signal, in addition to the evaluation of fluorescence lifetime using the FLIM-mode [19]. Modern scanning technology allows the registration and reconstruction of a number of consecutive equidistant depth-planes by implementing the principle of tomographic recording, this being termed multiphoton tomography.

MPT approaches to studying brain tissues provide the following specific features: the possibility to study specimens *in vivo* (specimen excision is not required); noninvasiveness (safety of low-intensity pulsed infrared laser radiation); the possibility of simultaneous monitoring of several parameters (SHG, TPEF and FLIM) and the possibility of three-dimension monitoring of changes in real-time and at high spatial resolution. The fluorescence of endogenous fluorophores can be reconstructed in three dimensions without previous preparation of the tissues. Previously [20], we have demonstrated that during the investigation of experimental gliomas with TPEF it is possible to differentiate tumor parenchyma and non-tumor cells in the perifocal area. Other studies of brain tissues using the MPM method in TPEF mode *in vivo* have shown its ability to visualize the vasculature and capillary system, and the ability of MPT to differentiate various types of neurons in the cortex [21–24].

OCT is based on the use of scattered low-intensity near-infrared light (wavelengths in the range from 700 to 1,300 nm) where determination of the tissue structure is performed by measuring the time needed for wave propagation from the emitter to the structural tissue components and back to the receiver. For clinical use in neurosurgery, OCT can be integrated into surgical microscopes and neuroendoscopes [25–27].

The spatial resolution of OCT (unlike MPT) cannot provide subcellular visualization and differentiation between benign and malignant brain tumors. Qualitative evaluation of images and the differentiation criteria in this case are based on the intensity and heterogeneity of the OCT signal, and the rate of its attenuation [17, 28].

The main trend in the development of OCT is enhancement of the methods of optical and further electronic processing of the OCT signal. For example, polarization-sensitive OCT [29] and, as applied by ourselves, cross-polarization OCT (CP OCT) allows for the detection of the polarization and/or cross-scattering properties of the tissue under investigation as a result of the presence of anisotropic structures (for instance, collagen) [30]. The possibility to study the different structural components of tissues in several OCT modes testifies to the ability of the method to considerably broaden the opportunity to apply it to neurosurgery, in particular [31].

Comparison of the different methods of *in vivo* visualization of microscopic objects is needed to determine the most advantageous ones to use to solve specific diagnostic tasks in the case of oncological diseases such as the identification of a tumor within a specimen, the determination of its grade of malignancy, or to identify the boundary between the tumor and normal tissue before its resection, and for the screening of the boundaries after such an operation.

The aim of the study was to analyze the first results of a parallel *ex vivo* study of glial tumors using MPT and CP OCT in order to determine their applicability in diagnostics.

Materials and Methods

Experimental model of glioblastoma. The object of study was the rat glioblastoma 101.8 model, obtained and maintained at the Research Institute of Human Morphology of the Russian Academy of Sciences (Russia) [32]. The choice of this model was based both on its morphological similarity to human glioblastomas and on the fact that the tumor is chemically induced and, therefore, has much in common with human perifocal area tissue (brain tissue at the edge of the tumor).

The work was performed on 5 female Wistar rats inoculated with glioblastoma 101.8. The tumor was transplanted in the Research Institute of Human Morphology of the Russian Academy of Sciences using standard methodology. The MPT and CP OCT investigations were performed on days 10–12 after the transplantation, when the tumor had formed and was growing intensively. The animals were excluded from the study by the method of cervical dislocation. The brain was

extracted, placed under the probe of a multiphoton optical coherence tomograph, and CP OCT images of the tumor and of the cortex immediately adjacent to the tumor were recorded.

The work with animals was guided by the "Regulations on Work with Experimental Animals" and the "International Recommendations for Medical-Biological Studies with Animals" [33], in addition to the ethical principles stated by the European Convention for the protection of vertebrate animals used for experimental and other scientific purposes (accepted in Strasburg on 18 March 1986 and approved in Strasburg on 15 June 2006) were carefully observed. The Ethical Committee of the Privolzhsky Federal Research Medical Centre of the Ministry of Health of the Russian Federation approved the experiments on animals.

Glial tumors from patients. Biopsy specimens of tumor tissue were obtained from 6 patients as a result of microsurgery and glial tumor excision. Optimal access was selected, taking into account the location of eloquent areas of the brain using frameless neuronavigation and intraoperative neurophysiological monitoring. In addition to the tumor itself, in the area of access to the tumor focus, we determined and sampled using tumoral pincers the perifocal tumor zone (tissue at the edge of the tumor resection which is usually to be coagulated) using tumoral pincers. The biopsy specimens were placed on pads moistened with saline solution and delivered within 2 h for investigation with CP OCT and MPT. For our experimental studies on human *ex vivo* samples we obtained approval from the Ethical Committee of the Privolzhsky Federal Research Medical Centre of the Ministry of Health of the Russian Federation.

Multiphoton tomography. The study was performed with an MPTflexCARS (JenLab, Germany) multiphoton tomograph on un-fixed specimens, *ex vivo*, without any special specimen preparation. The source of excitation radiation was an MAI TAI (Spectra Physics, USA) short-impulse femtosecond laser with an impulse repetition rate of 80 MHz and duration of 100 fs. The un-fixed specimens were observed through 170-micron cover glasses. The images were obtained using a 40x oil immersion objective with a numerical aperture of 1.3, which allowed a field of 250×250 μm (1024×1024 pixels) with a pixel resolution of 240 nm. To visualize the TPEF, mainly from NAD(P)H (nicotinamide adenine dinucleotide (phosphate)), we selected an optimal excitation wavelength of 750 nm. Detection was performed simultaneously in two channels at a wavelength of 409 nm by using a dichroic mirror and filters of 373–387 nm and 409–660 nm. The TPEF images of brain tissues were recorded in sequence until a depth of 100 μm was reached, with the distance between each focal plane being 5 μm. TPEF signal was visualized from the center of the tumor and from the perifocal zone of interest.

In total we obtained and analyzed 292 MPT images: 41 images of the cerebral hemispheres immediately adjacent to the tumor and 53 images of glioblastoma 101.8 from the rat specimens, and 68 images of the perifocal zones, 54 images of pilocytic astrocytoma (Grade I) and 76 images of glioblastoma (Grade IV) from the patients' specimens.

Qualitative evaluation of cellular density in MPT images. According to the recordings of a series of MPT images at equidistant depths we performed a 3D reconstruction of the tissue. The qualitative evaluation of cellular density was performed by summing the number of nuclei in each of the analyzed focal planes and their further normalization in the volume where they had been detected. The volume was calculated by multiplying the values of the length, width and height (the distance between the adjacent planes) of the image, all values being expressed in μm). This approach is more informative in respect of the evaluation of cellular density compared to the generally accepted histological methods, as it provides a calculation, not only for one selected plane, but for the whole object. The number of cells in each focal plane of the MPT images was calculated using Image J (NIH, USA) software [34, 35].

Cross-polarization optical coherence tomography. To obtain CP OCT images we used a device for high-speed spectral multimodal OCT (Institute of Applied Physics of the Russian Academy of Sciences, Russia) in CP OCT mode. The device works in angiographic mode and can evaluate the state of the microvasculature, which is important in *in vivo* studies [31].

The principle of operation and the technical characteristics of a CP OCT device have been described in detail in [36]. The central wavelength of the CP OCT system is 1,310 nm, spectral width 100 nm and optical power 20 mW. The depth-wise spatial resolution of the device is ~10–15 μm, the cross-sectional resolution is ~25 μm; the depth of scanning is ~1.7 mm; while the size of the obtained CP OCT image is 4×4 mm.

In total we obtained and analyzed 67 CP OCT images: 20 images of the rat brains (10 images of glioblastoma 101.8 and 10 images of the cortex near the tumor); plus 47 images of the patient tumors and perifocal zones.

Histological investigation. To verify the structure of the nervous tissue in the CP OCT and MPT images we studied the specimens histologically using hematoxylin and eosin staining. Histological specimens were observed under a Leica DM 2500 microscope in transmitted light and were photographed with a Leica DFC 245C (Leica Microsystems, Germany) digital camera. For the analysis we selected histological sections from the central part of the specimens (tumor and perifocal zone), which coincided with the plane of the obtained CP OCT images (zone of scanning) and had been marked with histological ink on the specimens during the investigation.

Results

MPT and CP OCT investigation of the rat glioblastoma 101.8 model. In Figure 1 we show typical MPT and CP OCT images of glioblastoma 101.8 and the cerebral cortex of a rat brain immediately adjacent to the tumor. In this case we compared the images of the

tumor and the grey matter, because the glioblastoma inoculated inside the ventricular system grew into the brain tissue and also reached the surface. The tumor was about 0.5 cm in diameter and was visually distinguishable from the cortex around it, so we could study both types of tissue. The rat cortex area was also chosen in order to match the mode of investigation with the MPT method, and to determine the depth of visualization at which the TPEF signal was sufficient for quantitative analysis of the image, i.e. for the development of further investigations.

During visualization of the cerebral cortex of rats' brains using the MPT method the TPEF signal is considerably reduced at a depth of about 80±10 μm. The corresponding histological specimens show that at this level the external, molecular layer of the brain with a thickness of 90.58±5.12 μm ends (Figure 1 (g)).

In a typical MPT image of the molecular cortex layer of a rat there are (Figure 1 (h)) tessellated individual neurons. The neuron nuclei are mostly oval, and are visualized in areas with no signal, surrounded with cytoplasm in the form of small granules that allow determination of the size of the nuclei [16]. The average nuclear perimeter was 15±3 μm, and the cross-sectional area — 12±5 μm^2. To characterize the oval nuclei it is more objective to simultaneously evaluate their cross sectional areas and their perimeters than to choose only one parameter for measurement [37]. But for neurons the MPT images show only a weak signal from the intercellular space and this correlated with the data from other MPT studies [16].

It should be noted that in the histological specimens of the cerebral cortex immediately adjacent to the tumor, pycnosis could be detected in a number of the neuron nuclei, while there were also poorly expressed pericellular and perivascular edemas (Figure 1 (f)) which could be the result of their proximity to the tumor.

The tumor tissue shows fundamentally different cytoarchitectonics. Morphological analysis of the glioblastoma 101.8 specimens showed

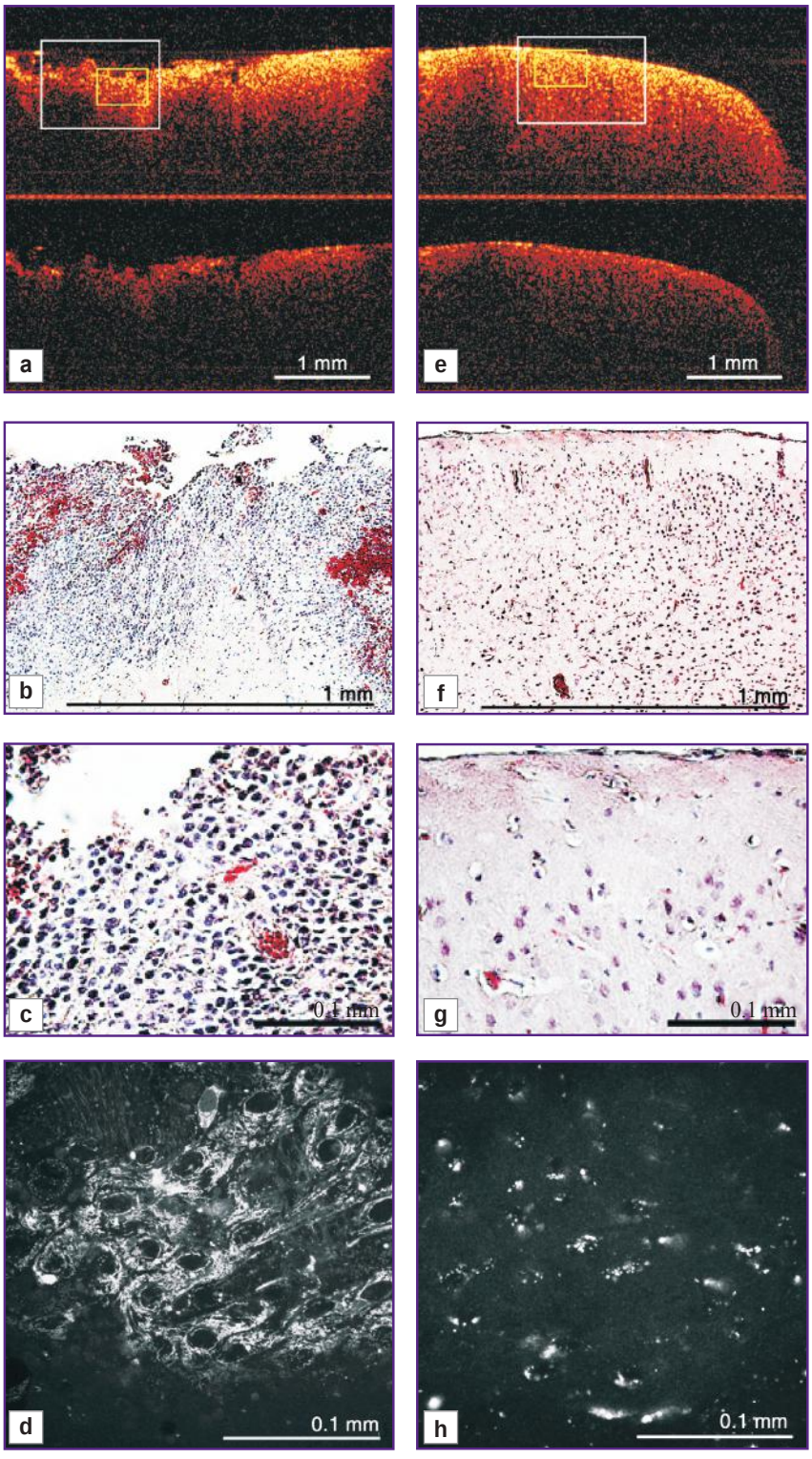

Figure 1. Rat glioblastoma 101.8 (a)–(d) and the cerebral cortex immediately adjacent to the tumor (e)–(h). Comparative study with MPT methods in two-photon excitation autofluorescence mode with an excitation wavelength of 750 nm and detection in the range 409–660 nm (d), (h), and CP OCT (a), (e): in co-polarization — upper part of the image; in cross-polarization — lower part of the image. White rectangle — area, corresponding to histological images (b), (f); green rectangle — area, corresponding to histological images (c), (g). The histological specimens (c), (g) contain the area from which the MPT images were obtained. Histologically stained with hematoxylin and eosin

that, at the time of investigation (days 10–12), the tumor demonstrated the signs of a mature glioblastoma, similar to a human glioblastoma, and was represented by a dense clusters of poorly differentiated cells all of approximately the same size and with only with rare foci of necrosis, infiltrative growth into the surrounding white matter. The tumors showed microvascular proliferation and small hemorrhages (Figure 1 (b), (c)). In MPT images the tumor tissue can be seen as densely located extended oval cells with a high intensity homogenous signal from all parts of their cytoplasm. There are signs of nuclear polymorphism and increased cellular density (Figure 1 (d)). The average cross sectional area of the cellular nuclei is 170±49 μm^2 while the perimeter is 51±7 μm. At some depths we can see the walls of tumor vessels, appearing as thin parallel lines.

Quantitative evaluation of the MPT images showed a considerable increase in cellular density in the tumor tissue: 2.5 times greater than that in the molecular layer of the rat cerebral cortex adjacent to the tumor (Figure 2). These finding were compared with the results of measurements of cellular density formed in the experimental tumors in rat brains where the equivalent correlation was 1.7 times [38].

In the CP OCT image in the region of the rat cerebral cortex near the tumor in co- and cross-polarizations there is a homogeneous OCT signal which is brighter on the surface; the signal decay rate is low (Figure 1 (e)). This characteristic of the signal reflects the morphological structure of the cerebral cortex. The external molecular layer (that gives a higher signal in cross-polarization) is characterized by a lower density of neurons but a larger number of neuron fibers, while, in the lower layers, the situation is reversed: the density is higher when there are fewer fibers (See Figure 1 (g)).

The OCT-signal from glioblastoma 101.8 in co-polarization is heterogeneous (an irregular distribution

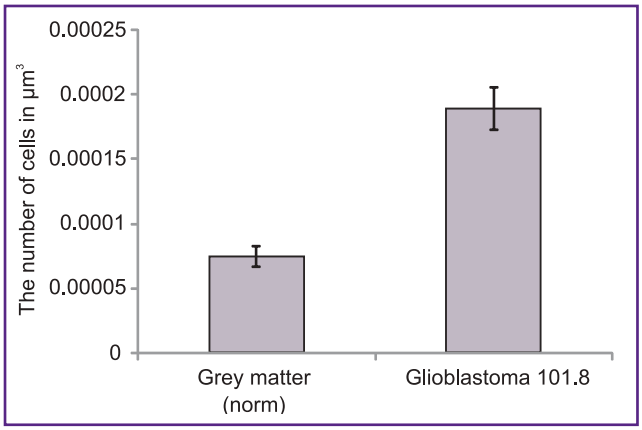

Figure 2. Quantitative analysis of the density of cellular nuclei in MPT images of the cortex immediately adjacent to the tumor, and of glioblastoma 101.8 *ex vivo* specimens of a rat brain. The values of the number of cells are standardized per volume; p<0.000003

of the high-level signal and its marked reduction), while the decay rate of the probing radiation varies along the transverse coordinate (Figure 1 (a), upper image). The OCT signal had a similar feature in cross-polarization, though the intensity was significantly lower (Figure 1 (a), lower image). The signal heterogeneity might be caused by the irregular structure of the tumor tissues which had clusters of tumor cells, tessellated necrosis and small hemorrhages (See Figure 1 (b)). We suggest that in this type of tumor (poorly differentiated tumor) the cells have an increased level of scattering while the areas with a low level of OCT signal correspond morphologically to the foci of necrosis and the hemorrhages.

Thus, MPT investigation of the cerebral cortex and rat glioblastoma 101.8 has helped to indicate that at excitation wavelengths of 740–760 nm in TPEF mode the optimal depth of the signal, at which there is little loss of quality and where it remains suitable for quantitative processing and comparison, is 90 μm for the cerebral cortex, and 70 μm for glioblastoma 101.8, due to the optical density of the latter. We obtained MPT images for the brain areas under study, and comparison of these images with the histological specimens allowed identification of the visual criteria for each type of MPT image.

CP OCT study of mature rat glioblastoma and of the cerebral cortex immediately adjacent to the tumor showed differences in the character of the OCT signals from these areas: heterogeneity of the signal, with a range of decay rates of the probing radiation along the transverse axis being typical of the tumor; a homogeneous signal which is brighter on the surface, with the same depth of penetration of the probing radiation along the transverse axis and a low decay rate of the signal are typical of the surrounding tissues (the cortex). This difference in signals allows identification of the tumor boundary visually.

MPT and CP OCT investigation of operative biopsies of brain tumors. We analyzed 18 specimens of operative biopsies of different grades of malignancy: 1 patient with pilocytic astrocytoma (Grade I), 3 specimens; and 5 patients with glioblastoma (Grade IV), 15 specimens.

The main morphological sign of *gliomas with low grade malignancy (Grade I)* that distinguish this grade of glioma from the white matter on the border of the tumor resection is the cellular density (Figure 3 (b)) which can be assessed visually in the corresponding MPT images (Figure 3 (d)). Comparative quantitative analysis of the MPT images of the white matter, the perifocal zone and the astrocytoma showed the difference in cellular density per unit of tissue volume was 1.8 times (Figure 4).

CP OCT images in co-polarization obtained from the pilocytic astrocytoma (Grade I) (Figure 3 (a), upper image) and the perifocal zone (Figure 3 (e), upper image) differ in the depth of signal decay, which is higher in the case of the astrocytoma. However, it is difficult to differentiate these images according to the degree of heterogeneity and the level of the OCT signal. The signal from the tumor tissue in cross-polarization has some heterogeneity in

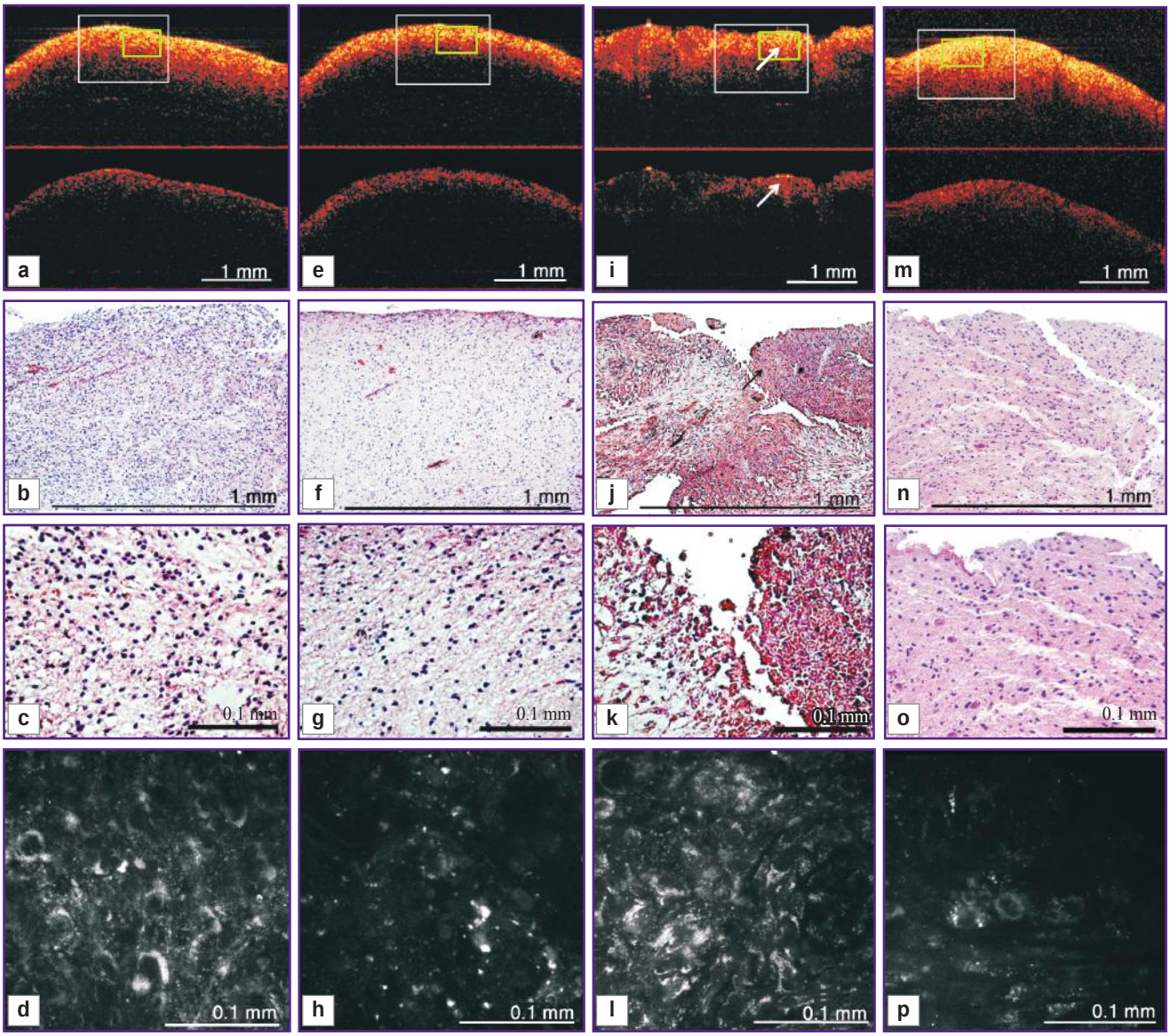

Figure 3. CP OCT, MPT and the corresponding histological images of *ex vivo* specimens of the human brain: pilocytic astrocytoma (Grade I) (a)–(d); glioblastoma Grade IV (i)–(l) and white matter at the edge of the tumor resection (e)–(h), (m)–(p). CP OCT-images (a), (e), (i), (m): in co-polarization — upper part of the image; in cross-polarization — lower part of the image. White rectangle — area, corresponding to histological images (b), (f), (j), (n); green rectangle — area, corresponding to histological images (c), (g), (k), (o). White and black arrows — the area of necrosis. Histological specimens (c), (g), (k), (o) contain the area from which the MPT images were obtained. Histologically stained with hematoxylin and eosin

the signal decay along the transverse axis (Figure 3 (a), lower image). One can suppose that the signal in this case is normally created by myelin fibers but that these are almost absent from the tumor tissue due to their destruction, and that the OCT signal evidently appears due to cross-scattering by the multiple cellular processes that form the tumor matrix.

Morphologically *gliomas with a high degree of malignancy (Grade III–IV)* are characterized by high cellular densities and nuclear polymorphism. These signs are clearly visible in the MPT images (Figure 3 (l)). Moreover, in the MPT images of the Grade IV glioblastoma the signal from the cytoplasm of the tumor cells is more intense. These signs in the MPT images are common both to the experimental rat model and the human tumor. In MPT images, Grade IV tumors can show such signs as microvascular proliferation and areas of necrosis [16]. These areas of necrosis in MPT images appear as heterogeneous distributions of granules of different intensity across the whole field of vision, while a more orderly signal from the cytoplasm of some cells is rare. The MPT image of the perifocal area (Figure 3 (p)) shows the high intensity of the fluorescence signal from the cellular organelles whereas there is no signal from the

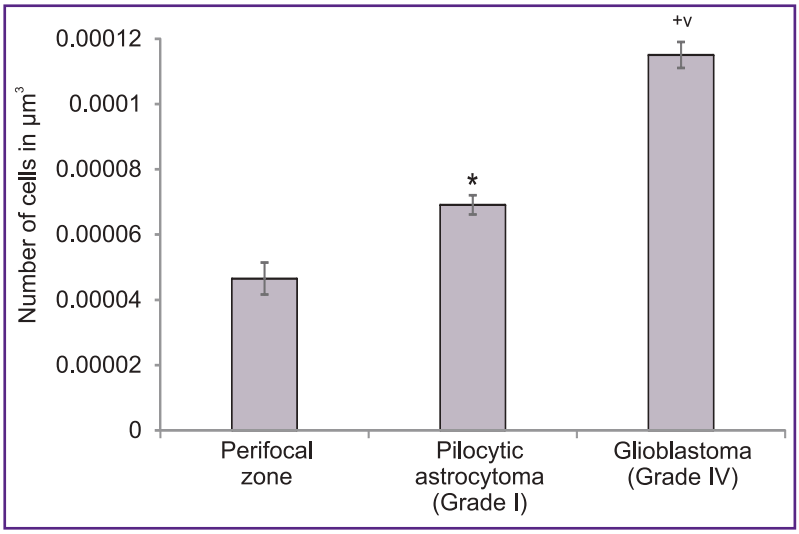

Figure 4. Density of cellular nuclei in tumor tissues and in the white matter of the perifocal zone. *Ex vivo* specimens from patients' brains: perifocal zone, pilocytic astrocytoma (Grade I) and glioblastoma (Grade IV). The values of the number of cells are standardized per volume. * Statistically relevant difference between perifocal zone and pilocytic astrocytoma, $p<0.000003$; $^{+}$ between perifocal zone and glioblastoma, $p<0.0000003$; ^{v} between glioblastoma and pilocytic astrocytoma, $p<0.000001$

nuclear areas or from the intercellular space. The cells are located at some distance from each other and this testifies to the tissue edema. (Figure 3 (o)).

The heterogeneity of the CP OCT images obtained from Grade IV tumor tissue in co-polarization is their specific feature (Figure 3 (i), upper image), which is evidently caused by the chaotically located light scattering elements in the tissue — alternating areas of increased cellular density and necrosis as are seen on the histological specimen (Figure 3 (j)). In CP OCT images in cross-polarization the signal is also heterogeneous, but it is noteworthy that there are areas with significantly reduced signal intensity or its complete absence (Figure 3 (i), upper image). This visually differentiates CP OCT images of Grade IV glioblastoma from those of the white matter of the perifocal zone (Figure 3 (m), lower image) and it is highly probable that this is connected with a virtual absence of anisotropic structures in this area of the tumor tissue.

CP OCT images of the white matter around the tumor in co- and cross-polarizations are, on the contrary, characterized by a homogeneous, highly intense signal in co-polarization with a low decay rate (See Figure 3 (m), lower image), which is most likely the result of the edema. On the histological specimens there are no changes in the fibrous structures of the nervous tissue, but the distance between them is increased, which is a sign of tissue edema (Figure 3 (n)). It can therefore be suggested that the edema contributes to greater depth of penetration of the probing radiation [39].

Summarizing the results of this part of the study it can be noted that human glioblastoma (Grade IV) has explicit structural specificity at both tissue and cellular levels, which determines the potentially high sensitivity of the MPT and CP OCT methods for differential diagnostics related to it. Astrocytomas (Grade I) are more difficult to analyze, as they have a high degree of cellular differentiation, lower cellular density and no nuclear polymorphism.

The studies demonstrated the significant potential of each method, indicating that for complex evaluation of the state of brain tissue it is desirable to use MPT and CP OCT together, as they complement one another in resolution, the field of vision and in their relatively deep visualization of tissues.

These pilot studies will help to develop a protocol for the combination of MPT and CP OCT to evaluate brain tissue, a protocol that offers a choice of optimal parameters of excitation for MPT studies (wave length, excitation power, and signal reception range) among the almost unlimited possibilities of the method itself and the optimization of the time of data collection.

Discussion. The development of optical methods of intraoperative diagnostics is a priority in neurosurgery, as it allows for considerably increasing the accuracy of surgical operations. In evaluating the potential of using confocal microscopy for this purpose one should mention the studies [40, 41], which show that it is possible to visualize the main diagnostic signs of glioblastomas, such as high cellular density, areas of necrosis, mitotic figures and microvascular proliferation with an endoscopic confocal microscope. However, this method has poorer resolution and depth of penetration when compared with MPT and MPM, as it uses one-photon excitation in the visible range, and not two-photon IR radiation as in MPT and MPM.

Kantelhardt et al. [42] used MPM for structural and photochemical *ex vivo* visualization of an experimental glioma and for human glial tumors. The authors showed the potential of this method for visualization of the tumor area and its boundaries with normal brain tissue at a cellular resolution. Quantitative evaluation of the density of the cellular nuclei enables the MPM data to be objective: this parameter is consistently higher in tumor tissue compared to the normal values. [38]. These findings regarding cellular density in the glioblastoma model and in the biopsy specimens of brain glioblastomas correlated with the results of measurements performed to determine the difference between normal and tumor tissues obtained by Kantelhardt et al from their patients [20].

The OCT method, unlike MPT, is mainly aimed at evaluation of the structure of the tissue being observed. According to the reference sources, the resolution

capacity of OCT is sufficient to determine the area of tumor infiltration where there are specific changes in the scattering properties compared with healthy brain tissue [28]. Our results showed that visually the signal from glial tumors in the OCT images in co-polarization looks heterogeneous in comparison with the homogeneous signal of the brain tissue from the perifocal zone, and this correlates with the data from other studies [17]. However, we consider that the most important characteristic of such an image is actually the differing decay rate of the signal deep in the tissue. Morphologically, glial tumors are characterized by high cellular density, irregular location of neurons/glia, and the presence of necrosis and hemorrhages, all of which can have an impact on the signal decay rate with depth, and result in an irregular distribution of the signal across the image.

This work has been the first time that OCT images have been obtained from *ex vivo* specimens of both glial tumors and the perifocal zones of human brain tissue in cross-polarization mode. The preliminary analysis of the results shows that, in the case of glioblastoma (Grade IV) with necrosis foci and blood circulation impairments, the signal is heterogeneous. The general reduction in the signal level in the case of brain tumors observed in cross-polarization may be connected with the considerably reduced amount of myelin in the damaged tissue. Edema of the tissue generally increases the depth of visualization in co-polarization, but reduces the signal level; in cross-polarization, edema also contributes to a reduction of cross-scattering.

CP OCT images of Grade I tumors and the surrounding perifocal zone are similar in general, so this does not allow for identifying any key peculiarities of the images to differentiate between these two states. To enable a more objective and rapid interpretation of images we are planning to widen the studies: to increase the number of groups and the number of specimens in each group, as well as to develop the methods for quantitative evaluation of CP OCT signals to take into account the potential for intraoperative implementation of the method [43]. Our article [36] was devoted to a more detailed review of the variants of CP OCT images of brain tumors with different grades of malignancy and to an explanation of the ways in which some morphological structures affect the OCT signal in cross-polarization.

The results allow us to compare MPT and CP OCT methods from the point of view of their effectiveness in clinical practice, by considering the benefits and drawbacks of each.

The main advantages of MPT are high spatial resolution (about 100 nm), non-invasiveness when the images are obtained through the use of probing IR radiation. The images can be obtained in near real-time if no supplementary contrasting is used. However, when pixel resolution is increased, based on the approach of scanning imaging, the time delay can increase up to tens of seconds. The particular advantage of MPT is its multimodality, i.e. the possibility to register TPEF for different excitation wavelengths that can excite different fluorophores. Using spectral selection one can register not only the TPEF from various fluorophores, but also the SHG signal from anisotropic media. A supplementary FLIM module can provide an analysis of the fluorescence lifetimes.

In this work we established that an effective depth for obtaining MPT images in TPEF mode is 80±10 μm. We think this is sufficient to determine the morphological structure of tissues in the operating theater, as well as to evaluate histological specimens, the thickness of which is 5–10 μm on average. While histological analysis requires the use of special stains for different tissue structures, which increases the number of specimens needed and makes the comparison of the same objects in different sections difficult, the MPT method, on the contrary, allows us to obtain information immediately about the morphology and functional activity of the same structures, thereby accelerating and facilitating the interpretation of results.

In comparison with MPT, the advantages of CP OCT are: a higher rate of data recording (several seconds) and a larger scanning area (up to 4×4×1 mm). The device also works in real-time mode, is non-invasive and has a high spatial resolution (about 10 μm), while special preparation of *ex vivo* objects is not required. The technique's multiple modes (cross-polarization, microangiography in real-time mode and elastographic tissue investigation) allow for obtaining a wide spectrum of data. If we consider such characteristics as small size of the device, the need for special operating conditions and price, the advantage of CP OCT compared to MPT is evident. The device weighs about 6 kg, is portable, works in a wide range of air temperatures, does not depend on separate illumination and is cheaper.

Our comparison of these two non-invasive, high resolution, real-time methods — MPT and CP OCT — draws us to the conclusion that the CP OCT method is desirable for application in the initial stages of an investigation, to differentiate tumors and their surrounding tissues and to determine the resection boundaries. MPT analysis being the one with higher cellular resolution, although still lower than CP OCT in terms of resolution and the field of vision, can help in target evaluation of the line of the resection to be performed and in express-cytobiopsy.

The use of MPT and CP OCT methods in clinical practice can considerably reduce the time required for diagnostics. The development of corresponding special software packages including automatic quantitative processing for each type of image will be a further step in this direction.

Conclusion. The combination of MPT and OCT offer great potential for intraoperative diagnostics during the surgery of glial tumors. MPT is characterized by its high spatial resolution and could become a fully-fledged method for express-biopsy, because it allows visualization of all the diagnostically relevant structural elements of the tissues. Nevertheless, in its existing form, the possibilities

for its use in determining the boundaries of tumor invasion are limited due to its small scanning area, its relatively low speed and the need for special conditions in the operating theater. By contrast, the spatial resolution of CP OCT is sufficient to determine tumor infiltration, and the accuracy of the method increases when cross-polarization mode is used. The wide application of these methods in clinical practice requires more extensive studies to clarify the criteria for differentiation between the tumor and the surrounding tissues.

Study Finding. The study was funded through a grant of the Russian Scientific Foundation, No.16-15-10391. The work used a multimodal OCT-device developed and constructed under a grant from the Government of the Russian Federation, and the Ministry of Education and Science of the Russian Federation, contract No.14. B25.31.0015.

Conflicts of Interest. The authors declare no conflict of interest.

References

1. Kohler B.A., Ward E., McCarthy B.J., Schymura M.J., Ries L.A., Eheman C., Jemal A., Anderson R.N., Ajani U.A., Edwards B.K. Annual report to the nation on the status of cancer, 1975–2007, featuring tumors of the brain and other nervous system. *J Natl Cancer Inst* 2011; 103(9): 714–736, https://doi.org/10.1093/jnci/djr077.

2. Ostrom Q.T., Gittleman H., Farah P., Ondracek A., Chen Y., Wolinsky Y., Stroup N.E., Kruchko C., Barnholtz-Sloan J.S. CBTRUS statistical report: primary brain and central nervous system tumors diagnosed in the United States in 2006–2010. *Neuro Oncol* 2013; 15(Suppl 2): ii1–ii56, https://doi.org/10.1093/neuonc/not151.

3. Louis D.N., Perry A., Reifenberger G., von Deimling A., Figarella-Branger D., Cavenee W.K., Ohgaki H., Wiestler O.D., Kleihues P., Ellison D.W. The 2016 World Health Organization Classification of Tumors of the Central Nervous System: a summary. *Acta Neuropathol* 2016; 131(6): 803–820, https://doi.org/10.1007/s00401-016-1545-1.

4. Almeida J.P., Chaichana K.L., Rincon-Torroella J., Quinones-Hinojosa A. The value of extent of resection of glioblastomas: clinical evidence and current approach. *Curr Neurol Neurosci Rep* 2014; 15(2): 517, https://doi.org/10.1007/s11910-014-0517-x.

5. Sanai N., Berger M.S. Glioma extent of resection and its impact on patient outcome. *Neurosurgery* 2008; 62(4): 753–766, https://doi.org/10.1227/01.neu.0000318159.21731.cf.

6. Sanai N., Polley M.Y., McDermott M.W., Parsa A.T., Berger M.S. An extent of resection threshold for newly diagnosed glioblastomas. *J Neurosurg* 2011; 115(1): 3–8, https://doi.org/10.3171/2011.2.jns10998.

7. Anokhina Yu.E., Gaidar B.V., Martynov B.V., Svistov D.V., Papayan G.V., Grigorievsky D.I. Prognostic significance of surgery volume under fluorescent intraoperative diagnostic applications in patients with malignant brain gliomas. *Vestnik rossiyskoy voenno-meditsinskoy akademii* 2014; 1(45): 19–24.

8. Stummer W., Reulen H.J., Meinel T., Pichlmeier U., Schumacher W., Tonn J.C., Rohde V., Oppel F., Turowski B., Woiciechowsky C., Franz K., Pietsch T.; ALA-Glioma Study Group. Extent of resection and survival in glioblastoma multiforme: identification of and adjustment for bias. *Neurosurgery* 2008; 62(3): 564–576, https://doi.org/10.1227/01.neu.0000317304.31579.17.

9. McGirt M.J., Chaichana K.L., Gathinji M., Attenello F.J., Than K., Olivi A., Weingart J.D., Brem H., Quinoñes-Hinojosa A.R. Independent association of extent of resection with survival in patients with malignant brain astrocytoma. *J Neurosurg* 2009; 110(1): 156–162, https://doi.org/10.3171/2008.4.17536.

10. McGirt M.J., Chaichana K.L., Attenello F.J., Weingart J.D., Than K., Burger P.C., Olivi A., Brem H., Quinoñes-Hinojosa A. Extent of surgical resection is independently associated with survival in patients with hemispheric infiltrating low-grade gliomas. *Neurosurgery* 2008; 63(4): 700–707, https://doi.org/10.1227/01.neu.0000325729.41085.73.

11. Sanai N., Berger M.S. Extent of resection influences outcomes for patients with gliomas. *Rev Neurol (paris)* 2011; 167(10): 648–654, https://doi.org/10.1016/j.neurol.2011.07.004.

12. Lacroix M., Abi-Said D., Fourney D.R., Gokaslan Z.L., Shi W., DeMonte F., Lang F.F., McCutcheon I.E., Hassenbusch S.J., Holland E., Hess K., Michael C., Miller D., Sawaya R. A multivariate analysis of 416 patients with glioblastoma multiforme: prognosis, extent of resection, and survival. *J Neurosurg* 2001; 95(2): 190–198, https://doi.org/10.3171/jns.2001.95.2.0190.

13. Colditz M.J., Jeffree R.L. Aminolevulinic acid (ALA)-protoporphyrin IX fluorescence guided tumour resection. Part 1: Clinical, radiological and pathological studies. *J Clin Neurosci* 2012; 19(11): 1471–1474, https://doi.org/10.1016/j.jocn.2012.03.009.

14. Stummer W., Pichlmeier U., Meinel T., Wiestler O.D., Zanella F., Reulen H.J.; ALA-Glioma Study Group. Fluorescence-guided surgery with 5-aminolevulinic acid for resection of malignant glioma: a randomised controlled multicentre phase III trial. *Lancet Oncol* 2006; 7(5): 392–401, https://doi.org/10.1016/s1470-2045(06)70665-9.

15. Zehri A.H., Ramey W., Georges J.F., Mooney M.A., Martirosyan N.L., Preul M.C., Nakaji P. Neurosurgical confocal endomicroscopy: a review of contrast agents, confocal systems, and future imaging modalities. *Surg Neurol Int* 2014; 5: 60, https://doi.org/10.4103/2152-7806.131638.

16. Kantelhardt S.R., Kalasauskas D., König K., Kim E., Weinigel M., Uchugonova A., Giese A. In vivo multiphoton tomography and fluorescence lifetime imaging of human brain tumor tissue. *J Neurooncol* 2016; 127(3): 473–482, https://doi.org/10.1007/s11060-016-2062-8.

17. Böhringer H.J., Boller D., Leppert J., Knopp U., Lankenau E., Reusche E., Hüttmann G., Giese A. Time-domain and spectral-domain optical coherence tomography in the analysis of brain tumor tissue. *Lasers Surg Med* 2006; 38(6): 588–597, https://doi.org/10.1002/lsm.20353.

18. Assayag O., Grieve K., Devaux B., Harms F., Pallud J., Chretien F., Boccara C., Varlet P. Imaging of non-tumorous and tumorous human brain tissues with full-field optical coherence tomography. *Neuroimage Clin* 2013; 2: 549–557, https://doi.org/10.1016/j.nicl.2013.04.005.

19. Kantelhardt S.R., Leppert J., Krajewski J., Petkus N., Reusche E., Tronnier V.M., Hüttmann G., Giese A. Imaging of brain and brain tumor specimens by time-resolved multiphoton excitation microscopy ex vivo. *Neuro Oncol* 2007; 9(2): 103–112, https://doi.org/10.1215/15228517-2006-034.

20. Kantelhardt S.R., Leppert J., Kantelhardt J.W.,

Reusche E., Hüttmann G., Giese A. Multi-photon excitation fluorescence microscopy of brain-tumour tissue and analysis of cell density. *Acta Neurochir (Wien)* 2009; 151(3): 253–262, https://doi.org/10.1007/s00701-009-0188-6.

21. Grutzendler J., Yang G., Pan F., Parkhurst C.N., Gan W.-B. Transcranial two-photon imaging of the living mouse brain. *Cold Spring Harb protoc* 2011; 2011(9): pdb.prot065474, https://doi.org/10.1101/pdb.prot065474.

22. Fumagalli S., Coles J.A., Ejlerskov P., Ortolano F., Bushell T.J., Brewer J.M., De Simoni M.G., Dever G., Garside P., Maffia P., Carswell H.V. In vivo real-time multiphoton imaging of T lymphocytes in the mouse brain after experimental stroke. *Stroke* 2011; 42(5): 1429–1436, https://doi.org/10.1161/strokeaha.110.603704.

23. Kobat D., Horton N.G., Xu C. In vivo two-photon microscopy to 1.6-mm depth in mouse cortex. *J Biomed Opt* 2011; 16(10): 106014, https://doi.org/10.1117/1.3646209.

24. Wang K., Horton N.G., Xu C. Going deep: brain imaging with multi-photon microscopy. *Optics and photonics News* 2013; 24(11): 32–39, https://doi.org/10.1364/opn.24.11.000032.

25. Kantelhardt S.R., Finke M., Schweikard A., Giese A. Evaluation of a completely robotized neurosurgical operating microscope. *Neurosurgery* 2013; 72(Suppl 1): A19–A26, https://doi.org/10.1227/NEU.0b013e31827235f8.

26. Finke M., Kantelhardt S., Schlaefer A., Bruder R., Lankenau E., Giese A., Schweikard A. Automatic scanning of large tissue areas in neurosurgery using optical coherence tomography. *Int J Med Robot* 2012; 8(3): 327–336, https://doi.org/10.1002/rcs.1425.

27. Lankenau E., Klinger D., Winter C., Malik A., Müller H., Oelckers S., Pau H.-W., Just T., Hüttmann G. Combining optical coherence tomography (OCT) with an operating microscope. In: *Advances in medical engineering*. Springer Berlin Heidelberg; 2007; p. 343–348, https://doi.org/10.1007/978-3-540-68764-1_57.

28. Böhringer H.J., Lankenau E., Stellmacher F., Reusche E., Hüttmann G., Giese A. Imaging of human brain tumor tissue by near-infrared laser coherence tomography. *Acta Neurochir (Wien)* 2009; 151(5): 507–517, https://doi.org/10.1007/s00701-009-0248-y.

29. de Boer J.F., Milner T.E. Review of polarization sensitive optical coherence tomography and Stokes vector determination. *J Biomed Opt* 2002; 7(3): 359–371, https://doi.org/10.1117/1.1483879.

30. Kiseleva E., Kirillin M., Feldchtein F., Vitkin A., Sergeeva E., Zagaynova E., Streltzova O., Shakhov B., Gubarkova E., Gladkova N. Differential diagnosis of human bladder mucosa pathologies in vivo with cross-polarization optical coherence tomography. *Biomed Opt Express* 2015; 6(4): 1464–1476, https://doi.org/10.1364/BOE.6.001464.

31. Yashin K.S., Karabut M.M., Fedoseeva V.V., Khalansky A.S., Matveev L.A., Elagin V.V., Kuznetsov S.S., Kiseleva E.B., Kravets L.Y., Medyanik I.A., Gladkova N.D. Multimodal optical coherence tomography in visualization of brain tissue structure at glioblastoma (experimental study). *Sovremennye tehnologii v medicine* 2016; 8(1): 73–81, https://doi.org/10.17691/stm2016.8.1.10.

32. Khalansky A.S., Kondakova L.I. Transplanted rat glioma 101.8. I. Biological characteristics. *Klinicheskaya i eksperimental'naya morfologiya* 2013; 4(8): 63–68.

33. Senft C., Bink A., Franz K., Vatter H., Gasser T., Seifert V. IIntraoperative MRI guidance and extent of resection in glioma surgery: a randomised, controlled trial. *Lancet Oncol* 2011; 12(11): 997–1003, https://doi.org/10.1016/s1470-2045(11)70196-6.

34. Valdés P.A., Kim A., Leblond F., Conde O.M., Harris B.T., Paulsen K.D., Wilson B.C., Roberts D.W. Combined fluorescence and reflectance spectroscopy for in vivo quantification of cancer biomarkers in low- and high-grade glioma surgery. *J Biomed Opt* 2011; 16(11): 116007, https://doi.org/10.1117/1.3646916.

35. Sanai N., Snyder L.A., Honea N.J., Coons S.W., Eschbacher J.M., Smith K.A., Spetzler R.F. Intraoperative confocal microscopy in the visualization of 5-aminolevulinic acid fluorescence in low-grade gliomas. *J Neurosurg* 2011; 115(4): 740–748, https://doi.org/10.3171/2011.6.jns11252.

36. Yashin K.S., Gubarkova E.V., Kiseleva E.B., Kuznetsov S.S., Karabut M.M., Medyanik I.A., Kravets L.Y., Gladkova N.D. Ex vivo imaging of human gliomas by cross-polarization optical coherence tomography: pilot study. *Sovremennye tehnologii v medicine* 2016; 8(4): 14–22, https://doi.org/10.17691/stm2016.8.4.02.

37. Shubina O.S, Teltsov L.P., Komusova O.I. Cytological and morphometric features perednetemennoy neurons of the cerebral cortex of white rats. *Sovremennye problemy nauki i obrazovaniya* 2015; 2(1). URL: https://www.science-education.ru/en/article/view?id=19078.

38. Kantelhardt S.R., Leppert J., Kantelhardt J.W., Reusche E., Hüttmann G., Giese A. Multi-photon excitation fluorescence microscopy of brain-tumour tissue and analysis of cell density. *Acta Neurochir (Wien)* 2009; 151(3): 253–262, https://doi.org/10.1007/s00701-009-0188-6.

39. Rodriguez C.L., Szu J.I., Eberle M.M., Wang Y., Hsu M.S., Binder D.K., Park B.H. Decreased light attenuation in cerebral cortex during cerebral edema detected using optical coherence tomography. *Neurophotonics* 2014; 1(2): 025004, https://doi.org/10.1117/1.NPh.1.2.025004.

40. Eschbacher J., Martirosyan N.L., Nakaji P., Sanai N., Preul M.C., Smith K.A., Coons S.W., Spetzler R.F. In vivo intraoperative confocal microscopy for real-time histopathological imaging of brain tumors. *J Neurosurg* 2012; 116(4): 854–860, https://doi.org/10.3171/2011.12.jns11696.

41. Schlosser H.G., Suess O., Vajkoczy P., van Landeghem F.K., Zeitz M., Bojarski C. Confocal neurolasermicroscopy in human brain — perspectives for neurosurgery on a cellular level (including additional comments to this article). *Cent Eur Neurosurg* 2010; 71(1): 13–19, https://doi.org/10.1055/s-0029-1237735.

42. Kantelhardt S.R., Leppert J., Krajewski J., Petkus N., Reusche E., Tronnier V.M., Huttmann G., Giese A. Imaging of brain and brain tumor specimens by time-resolved multiphoton excitation microscopy ex vivo. *Neuro Oncol* 2007; 9(2): 103–112, https://doi.org/10.1215/15228517-2006-034.

43. Kut C., Chaichana K.L., Xi J., Raza S.M., Ye X., McVeigh E.R., Rodriguez F.J., Quiñones-Hinojosa A., Li X. Detection of human brain cancer infiltration ex vivo and in vivo using quantitative optical coherence tomography. *Sci Transl Med* 2015; 7(292): 292ra100, https://doi.org/10.1126/scitranslmed.3010611.